ADVANCED ELECTRONIC MATERIALS

Supporting Information

for *Adv. Electron. Mater.*, DOI: 10.1002/aelm.201700614

Photothermal-Induced Nanowelding of Metal–Semiconductor Heterojunction in Integrated Nanowire Units

*Pintu Ghosh, Jinsheng Lu, Ziyao Chen, Hangbo Yang, Min Qiu, and Qiang Li**

Supporting Information

Photothermal-induced nanowelding of metal-semiconductor heterojunction in integrated nanowire units

*Pintu Ghosh, Jinsheng Lu, Ziyao Chen, Hangbo Yang, Min Qiu, and Qiang Li**

1. Experimental setup

The experimental setup for nanowelding and electrical characterization is shown in Figure S1. A continuous-wave (CW) laser beam (of wavelength 532 nm) is used for nanowelding.

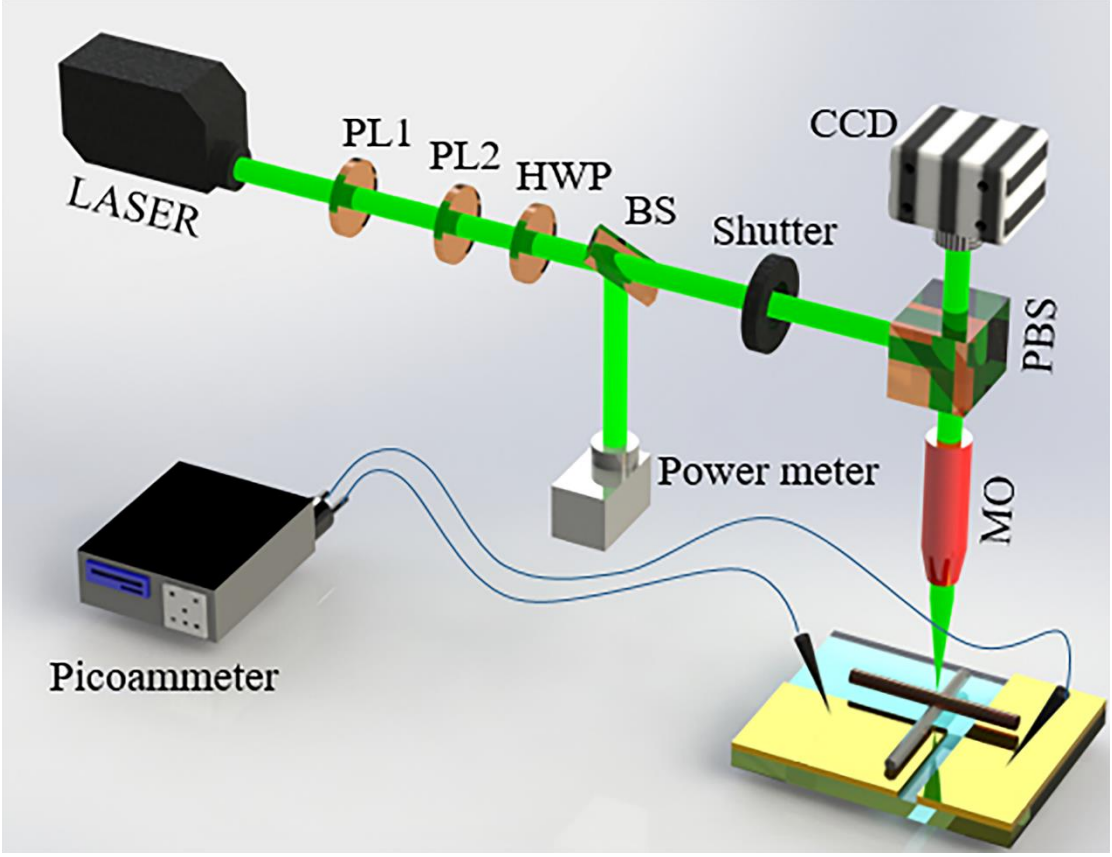

Figure S1 Experimental setup for nanowelding and electrical characterization. PL1 and PL2 are the polarizers, HWP is the half wave plate, BS is the beam splitter, PBS is the Pellicle beam splitter, and MO is the microscope objective.

The laser beam is focused on the target by a microscope objective (100 X, Mitutoyo Microscope). The combination of half-wave plate and two polarizers is used control the polarization and power of the incident laser beam. The mechanical shutter is used to manipulate the time of the laser shots. The smallest shot is of 2 ms. A three-dimensional translational stage attached with piezoelectric control (with smallest step size of 30 nm) is utilized for targeted welding. Two micro-tungsten probes connected with a picoammeter are used to obtain I-V characteristic curves.

2. Simulations to determine the optimum incident laser power corresponding to different incident laser beam polarization and orientation of the NWs

Fig. S2 (a) shows that the slope corresponding to the parallel incident laser beam (electric field is parallel to the long axis of the top NW) is less compared to the perpendicular (electric field is perpendicular to the long axis of the top NW) incident case.

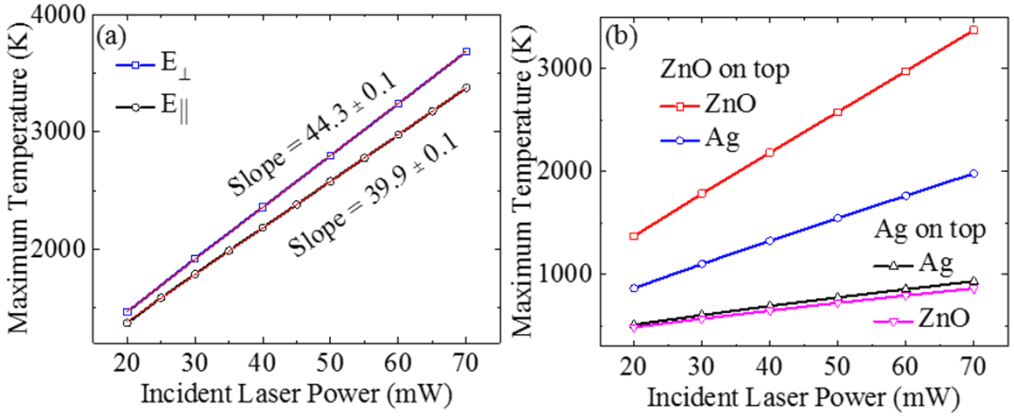

Figure S2 Maximum temperature versus incident laser power plots for different incident laser beam polarization (a) and orientation (b) of the NWs. The diameter and length of the NWs are kept fixed at 300 nm and 10 μm, respectively.

Therefore, it is easier to control the welding when the electric field of the incident laser is parallel to the long axis of the top NW. From Fig. S2 (b), it can be observed that it is possible to reach melting point of both ZnO and Ag NWs for the same incident laser power when ZnO NW is on top, whereas the same is not possible when the Ag NW is kept on top of ZnO NW. The corresponding electric field distribution for both these orientations are shown in Fig. S5.

3. Simulation results to determine the effect of length and diameter of the NWs

It can be observed from Fig. S3 that the maximum temperature increases linearly with incident laser power, and it requires more power to reach the same maximum temperature for longer or thicker NWs. These effects are same as in case when the Ag NW is on top, however the maximum temperature of the ZnO NW is much higher when the ZnO NW lies on top compared to the maximum temperature of the Ag NW when Ag NW is on top.

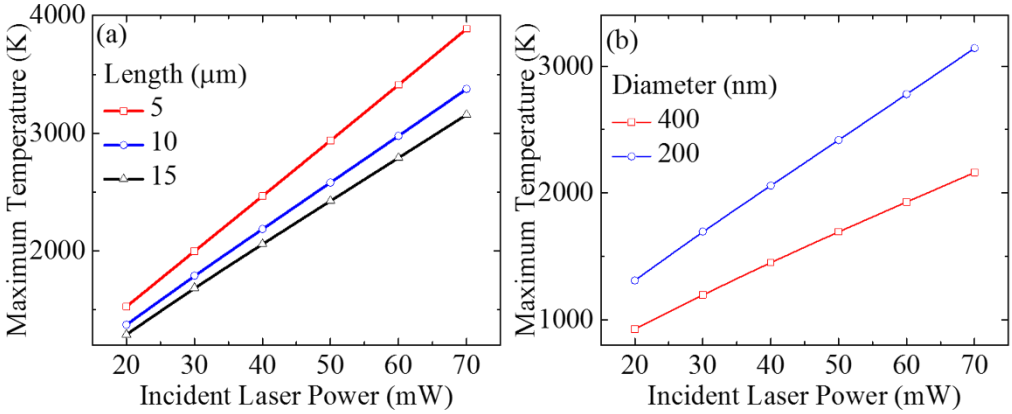

Figure S3 (a) Simulated results showing the variation of maximum temperature of ZnO NW corresponding to varying incident laser power and length of the ZnO NW when it lies on top of an Ag NW. The diameter of the NWs is kept fixed at 300 nm, and incident laser beam polarization is parallel. (b) Maximum temperature versus incident laser power plot corresponding to different diameter of the ZnO NW placed on Ag NW. The length of the NWs is kept fixed at 10 μm, and incident laser beam polarization is parallel.

4. Welding of Ag and ZnO NWs on Au electrodes

It has been observed that the current through the device is lower than a few nA (lower limit of the used ammeter) for the applied bias voltage ranging from -40 V to 40 V if the NWs are not welded on the Au electrodes. Therefore, apart from the welding of the junction of the NWs, the other ends of the NWs are also welded on the Au electrodes. The SEM images of the welded NWs on Au electrode show that the NWs melt and take hemispherical shape on Au electrode (see Fig. S4).

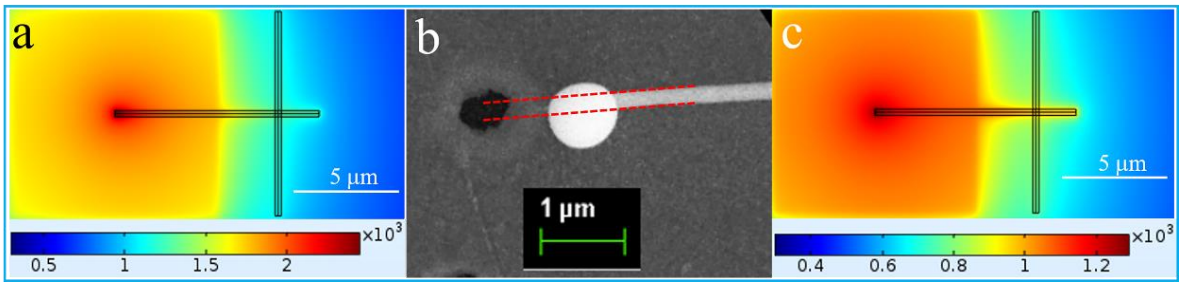

Figure S4 (a) Simulated temperature distribution plots for welding ZnO NW on Au electrode corresponding to laser power 70 mW. (b) SEM images of welded Ag NW on Au electrodes. The dashed red lines represent the orientation of the NWs before welding. (c) Simulated temperature distribution plots for welding Ag NW on Au electrodes corresponding to laser power 60 mW.

5. Electric field distribution corresponding to different orientation of the NWs and polarization of the incident laser beam

It can be observed from the electric field distribution at the end of the NWs that surface plasmon mode is excited on Ag NW, whereas waveguide mode is excited for ZnO NW (see Fig. S5).

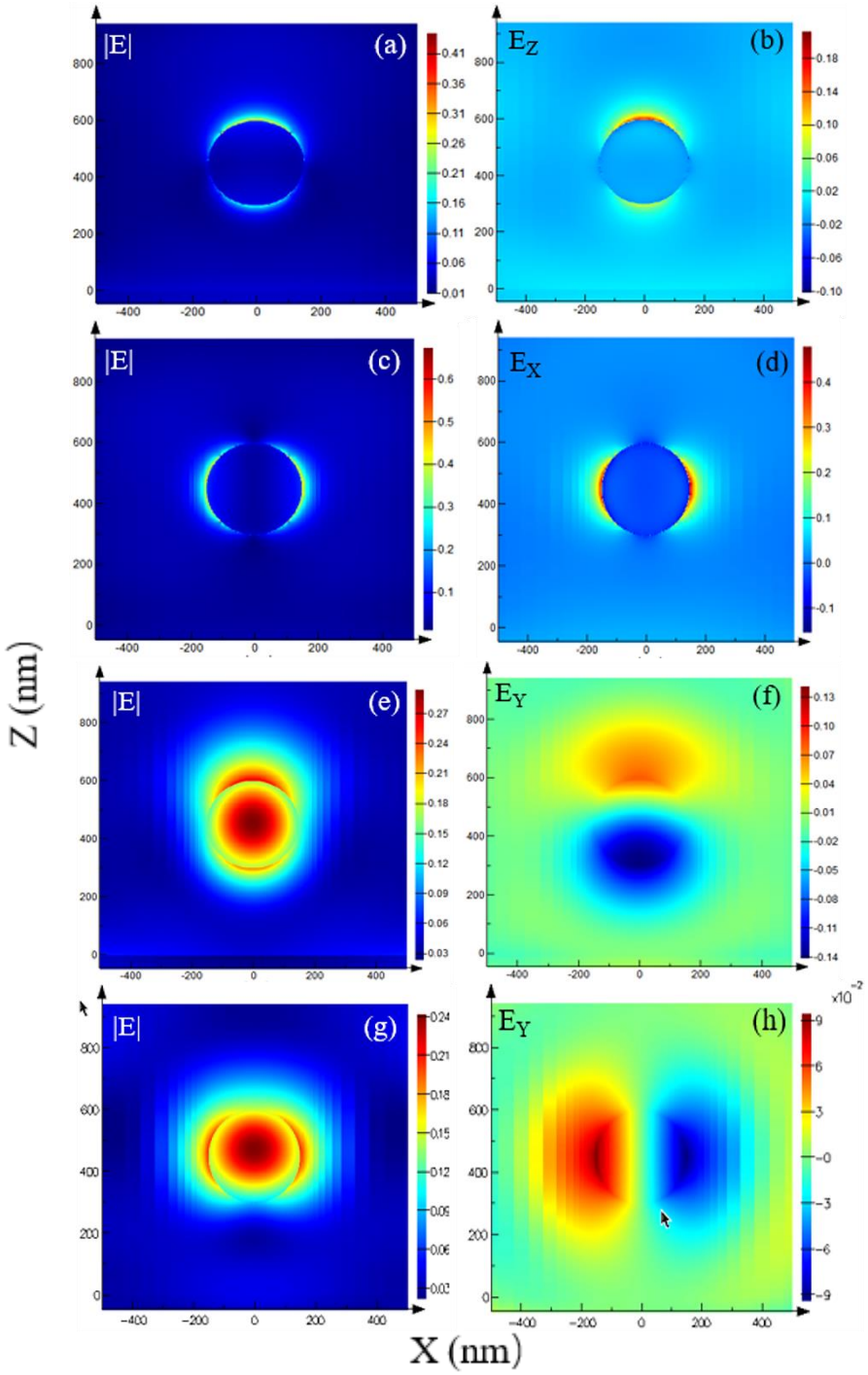

Figure S5 Simulated electric field distribution corresponding to different orientation of the NWs and polarization of the incident laser beam. Electric field distribution at the end of Ag NW (a-d) and ZnO NW (e-h) when Ag and ZnO NWs are on top, respectively. (a, c, e, and g) Electric field magnitude. (b, d, f, and h) Dominant electric field component. (a, b, e, and f) Corresponding to parallel, and (c, d, g, and h) for perpendicular polarization of the incident laser beam.